Resolution of the multichannel anomaly in the extraction of S-matrix resonance-pole parameters

Saša Ceci,[1,2,*] Jugoslav Stahov,[3,4] Alfred Švarc,[1] Shon Watson,[3] and Branimir Zauner[1]

[1]*Rudjer Bošković Institute, Bijenička cesta 54, P.O. Box 180, 10002 Zagreb, Croatia*
[2]*Department of Physics and Astronomy, University of Georgia, Athens, Georgia 30602, USA*
[3]*Abilene Christian University, ACU Station Box 27963, Abilene, Texas 79699, USA*
[4]*University of Tuzla, Faculty of Science, Univerzitetska 4, 35000 Tuzla, Bosnia and Herzegovina*

(Received 22 September 2006; published 20 June 2008)

Within the framework of a mathematically well-defined coupled-channel T-matrix model we have improved the existing multichannel pole-extraction procedure based on the numerical analytic continuation of the channel propagator, and for the first time we present the full set of pole parameters for already published amplitudes. Standard single-channel pole-extraction method (speed plot) was then applied to those amplitudes and resulting sets of T-matrix poles were inspected. The anomaly has been established that in some partial waves the pole values extracted using the standard single-channel methods differ not only from the values obtained using the analytic continuation method, but also change from one reaction to another. Inspired by this peculiarity, we have developed a new single-channel pole-extraction method based solely on the assumption of the partial wave analyticity. Since the speed plot turns out to be the lowest order term of the proposed method, the anomaly is understood and resolved.

DOI: 10.1103/PhysRevD.77.116007 PACS numbers: 11.55.−m, 14.20.Gk, 25.40.Ny

I. INTRODUCTION

The determination of the scattering matrix (S-matrix) is considered to be the major objective of both scattering theory and energy-dependent analysis of scattering data. The collection of S-matrix poles in the ''unphysical'' Riemann sheet is related to resonance mass spectrum [1,2] so obtaining them is the crucial goal of any partial-wave analysis. There is, however, a long lasting (and yet unresolved) controversy on the resonances' physical properties. It is not clear whether physical mass and decay width of a resonance are given by the ''conventional'' resonance parameters like Breit-Wigner mass and the decay width, or by resonance pole parameters—real part and $-2\times$ imaginary part of pole [3,4]. In the case of baryon resonances, the compromise is achieved in a way that conventional, as well as pole parameters, are collected in the Review of Particle Physics (RPP) [5].

In this paper, we present two methods for obtaining the resonance pole parameters from energy-dependent partial waves. The first method, built into the Carnegie-Mellon-Berkeley (CMB) formalism [6], is based on performing the analytic continuation of a channel propagator. Instead of using the tabulated values of the two-variable dispersion relations as it has been done in Ref. [7], we have improved the method by using the analytic continuation in a Pietarinen expansion form [8]. Using this method we have extracted a set of pole parameters for the partial-wave amplitudes of Ref. [7] and we show them here for the first time.

As a self-consistency test, we have applied the standard speed-plot technique (single-channel) to amplitudes of Ref. [7] which describe various different channel reactions and surprisingly obtained values which differed from those obtained when using the inherent analytic continuation method. In addition, the obtained parameters were not identical for different channel processes. This anomalous behavior challenged common sense, and the conclusion was drawn that either our partial-wave analysis or the applied pole-extraction methods were incorrect. The single-channel extraction methods were carefully examined and those methods were determined to be at fault. This effort resulted in a new model-independent extraction method free from this anomaly: the T-matrix *regularization method*. The new procedure is based on eliminating the simple pole and expanding the obtained regularized function at the pole energy in a Taylor series over the values on the real axis. The main quality of this method is that it is not restricted to CMB formalism, and all of the required information needed to use the proposed method lie on the real (physical) axis of the complex-energy plane—exactly where experiments provide data. When the new method is applied to the test amplitudes of Ref. [7], the discrepancies have disappeared and the set of poles obtained with the analytic continuation method is reproduced. Therefore we recommend this method over the usual model-independent methods (e.g. speed plot [3]) for obtaining resonance pole parameters.

To our satisfaction and surprise the standard speed-plot technique turned out to be just the lowest order approximation of the regularization method, so the root of the anomaly was found.

In addition, we calculated elastic pole residues and the obtained values were in quite good agreement with others published in the RPP [5]. Since there are still no RPP

*sasa.ceci@irb.hr

 © 2008 The American Physical Society

estimates for elastic residues, this result gives a convenient tool for creating them.

There is a number of alternative ways in which the pole parameters are presently extracted from the partial-wave amplitudes. Since we are focusing our interest on the quality of single-channel methods, speed plot in particular, we shall mention them only to acknowledge their existence.

Other encountered procedures are the N/D method and Flatté's method.

The N/D method is a technique in which the dispersion relations are used to construct the amplitudes in the physical region using the knowledge of the left-hand cut singularities. The idea is to represent the partial-wave amplitude as a ratio of two functions, the numerator is represented with a function N(s) which is analytic in the s plane on the left-hand cut only, and D(s) which is analytic on the right-hand cut only. The poles of the scattering amplitude are identified with the zeroes of the D(s), and the problem of extra zeroes is often difficult to solve. The method has been introduced a long time ago by Ref. [9], and since then it has been mostly used in meson physics, typically for cases when the knowledge about the left-hand cut is available [10,11].

Flatté's method, introduced in 1976 [12], is based on recognizing the fact that the partial-wave T-matrix experiences the presence of new channel openings and the effect is taken into account effectively by modifying the traditional Breit-Wigner form which is representing the resonant structure with additional, energy-dependent terms for the resonance width. The amplitude poles are extracted as the singularities of the modified Breit-Wigner function. The possible issue with Flatté's method is that it assumes that the partial-wave amplitude can be represented locally with a Breit-Wigner function.

We start our paper with a brief summary of the CMB formalism. After that, we present the improvement of the analytic continuation method, demonstrate the anomaly, introduce the regularization procedure, and finally demonstrate the disappearance of the single-channel speed-plot technique anomaly. The last section is devoted to the results and conclusions.

II. CORE OF THE CMB MODEL

Our current partial-wave analysis [7] is based on the CMB approach [6]. The most prominent property of this approach is analyticity of partial waves with respect to Mandelstam s variable. In every discussion of partial-wave poles, analyticity plays a crucial role since poles are situated in a complex plane, away from the physical region. Any knowledge about the nature of partial-wave singularities would be impossible to gain if partial waves were not analytic functions. The ability to calculate pole positions is not just a benefit of the CMB model's analyticity but also a necessity for the resonance extraction. In this approach, the resonance itself is considered to exist if there is an associated partial-wave pole in the unphysical sheet.

The central role of the CMB analysis belongs to the unitary-normalized partial-wave T-matrix $\mathbf{T}(z)$ [6,7,13]. It is a matrix in channel indices and generic complex variable z from now on denotes Mandelstam s. The connection between S-matrix and T-matrix is given by $\boldsymbol{S}(z) = \boldsymbol{I} + 2i\boldsymbol{T}(z)$ where $\boldsymbol{I}$ is the unit matrix. Two main ingredients of the model are the channel propagator $\mathbf{\Phi}(z)$ (the diagonal matrix in channel indices which takes care of channel related singularities) and the bare resonant propagator $\mathbf{G}_0(z)$ (the diagonal matrix in resonant indices incorporating real first-order poles related to resonances [and background]). Background contribution is given by two subthreshold poles (another pole may be placed further above the considered energy region). Dressed resonance propagator $\mathbf{G}(z)$ is given by the resolvent (Schwinger-Dyson) equation $\boldsymbol{G}^{-1}(z) = \boldsymbol{G}_0^{-1}(z) - \boldsymbol{\Sigma}(z)$, where self-energy term $\boldsymbol{\Sigma}(z)$ is built from the channel propagator as $\boldsymbol{\gamma} \cdot \mathbf{\Phi}(z) \cdot \boldsymbol{\gamma}^{\mathrm{T}}$. The parameter matrix $\boldsymbol{\gamma}$ is a nonsquare matrix obtained from the least-square fit to experimental or partial-wave data. In addition to $\boldsymbol{\gamma}$ parameter matrices, the values of the bare propagator real poles are concurrently acquired from the same fit. The partial-wave data are fitted by the unitary-normalized partial-wave T-matrix given by the relation

$$\mathbf{T}(z) = \sqrt{\mathrm{Im}\mathbf{\Phi}(z)} \cdot \boldsymbol{\gamma}^{\mathrm{T}} \cdot \mathbf{G}(z) \cdot \boldsymbol{\gamma} \cdot \sqrt{\mathrm{Im}\mathbf{\Phi}(z)}. \quad (1)$$

The channel propagator matrix $\mathbf{\Phi}(z)$ is assembled from channel propagator functions $\phi(z)$. The dominant singularity in the resonant region, apart from resonances themselves, is the physical (channel opening) branching point x_0. In the CMB approach, contributions from other singularities (left-hand cut, nucleon pole, etc.) are given partly by the design of the channel propagator imaginary part, while the rest is taken care of by the background.

Analyticity of the channel propagator function $\phi(z)$ is ensured by the once-subtracted dispersion relation

$$\phi(z) = \frac{z - x_0}{\pi} \mathrm{P} \int_{x_0}^{\infty} \frac{\mathrm{Im}\phi(x')dx'}{(x' - z)(x' - x_0)}, \quad (2)$$

where P stands for Cauchy principal value. The physical (unitarity) branch cut is, thus, chosen to go from the branching point x_0 to positive infinity. The variable x' is used in the integral rather than z' to indicate the integration path is on the real axis.

The form of the channel propagator imaginary part is given as

$$\mathrm{Im}\,\phi(x) = \frac{[q(x)]^{2L+1}}{\sqrt{x}\{Q_1 + \sqrt{Q_2^2 + [q(x)]^2}\}^{2L}}, \quad (3)$$

where $q(x)$ is the standard two-body center-of-mass mo-

mentum for a particular meson-baryon channel, Q_1 and Q_2 are the CMB model parameters with values equal to the π meson (or, in our case [7], the channel meson mass), and L is the orbital angular momentum number of the given partial wave.

III. EXTRACTION METHOD ONE: ANALYTIC CONTINUATION

From Eq. (3) it is evident that $\phi(z)$ has a square-root type singularity. Instead of calculating the dispersion integral (2) for each point in complex plane, we decided to use the expansion (similar to Pietarinen's in Ref. [8] or Ciulli's [14])

$$\phi_{\mathrm{I}}(z) = \sum_{n=0}^{N} c_n (Z_{\mathrm{I}}(z))^n, \tag{4}$$

where c_n are coefficients of expansion. The new channel dependent variable is given by its principal branch

$$Z_{\mathrm{I}}(z) = \frac{\alpha - \sqrt{x_0 - z}}{\alpha + \sqrt{x_0 - z}}, \tag{5}$$

with the tuning parameter α. This function is fitted to a data set consisting of imaginary parts of $\phi(x)$ from Eq. (3) and real parts of $\phi(x)$ calculated from dispersion relation (2), both of them evaluated at the real axis (hence x). The general idea is that the $\phi(z)$ inherits analytic structure from $Z(z)$. We obtained parameters α and coefficients c_n for each channel and for all analyzed partial waves. The least-square fit is considered to be good if it meets the following conditions: (i) small number of coefficients c_n needed (7 or 8, at most); (ii) the function fitted to the part of the data set, when extrapolated outside of the fitted region, is consistent with the rest of data; and (iii) fitting just the imaginary part of $\phi(x)$ produces real part that is in agreement with values obtained from (2).

The channel propagator given by expansion (4) is obtained quite accurately and works very well in the resonant region in the vicinity of the physical axis.

Every channel opening is responsible for two Riemann sheets: the first (physical) sheet with physical partial waves and the secondary (unphysical) sheet with resonant poles. To get to the unphysical sheet it is enough to use the second branch of $Z(z)$

$$Z_{\mathrm{II}}(z) = \frac{\alpha + \sqrt{x_0 - z}}{\alpha - \sqrt{x_0 - z}}. \tag{6}$$

Finally, it is evident from Eq. (1) that all poles of each partial wave must by construction be the same in all channels and, in fact, equal to the poles of the resolvent $\mathbf{G}(z)$.

In this paper, we use T-matrices obtained in our latest published partial-wave analysis [7]. We collect all the poles of $\mathbf{G}(z)$ obtained by analytic continuation method as columns three and four in Table I. Since this method gives poles of partial waves in Mandelstam s variable, comparison to RPP estimates is made with the square root of the Mandelstam pole (selecting branch with positive real part) denoted by μ.

TABLE I. The N^* resonance pole parameters obtained by the continuation along with RPP [5] estimates. The N/E term is given if a resonance pole position does not have a RPP estimate, while the $N(?)$ stands for resonances unnamed in the RPP.

	Review of Particle Physics [5] pole positions			Analytic continuation	
N^*	L_{2I2J}	Reμ (MeV)	-2 Imμ (MeV)	Reμ (MeV)	-2 Imμ (MeV)
$N(1535)$	S_{11}	1505(10)	170(80)	1517	190
$N(1650)$	S_{11}	1660(20)	160(10)	1642	203
$N(2090)$	S_{11}	N/E	N/E	1785	420
$N(1440)$	P_{11}	1365(20)	210(50)	1359	162
$N(1710)$	P_{11}	1720(50)	230(150)	1728	138
$N(?)$	P_{11}	N/E	N/E	1708	174
$N(2100)$	P_{11}	N/E	N/E	2113	345
$N(1720)$	P_{13}	1700(50)	250(140)	1686	235
$N(1520)$	D_{13}	1510(5)	115(5)	1505	123
$N(1700)$	D_{13}	1680(50)	100(50)	1805	130
$N(2080)$	D_{13}	N/E	N/E	1942	476
$N(1675)$	D_{15}	1660(5)	140(15)	1657	134
$N(2200)$	D_{15}	N/E	N/E	2133	437
$N(1680)$	F_{15}	1670(5)	120(15)	1664	134
$N(1990)$	F_{17}	N/E	N/E	1990	303
$N(?)$	G_{17}	N/E	N/E	1740	270
$N(2190)$	G_{17}	2050(100)	450(100)	2060	393

TABLE II. The N^* resonance pole parameters obtained by the analytic continuation method and speed plot in various channels. The $N(?)$ stands for resonances unnamed in the RPP.

Resonance		Analytic continuation		Speed-plot method					
				$\pi N \to \pi N$		$\pi N \to \eta N$		$\eta N \to \eta N$	
N^*	L_{2I2J}	$\mathrm{Re}\mu$ (MeV)	$-2\,\mathrm{Im}\mu$ (MeV)	$\mathrm{Re}\mu$ (MeV)	$-2\,\mathrm{Im}\mu$ (MeV)	$\mathrm{Re}\mu$ (MeV)	$-2\,\mathrm{Im}\mu$ (MeV)	$\mathrm{Re}\mu$ (MeV)	$-2\,\mathrm{Im}\mu$ (MeV)
$N(1535)$	S_{11}	1517	190	1506	83	1531	388	···	···
$N(1650)$	S_{11}	1642	203	1657	183	1601	208	1632	179
$N(2090)$	S_{11}	1785	420	1764	133	···	···	1917	423
$N(1440)$	P_{11}	1359	162	1355	154	ST[a]	ST[a]	ST[a]	ST[a]
$N(1710)$	P_{11}	1728	138	1722	121	1733	154	1679	151
$N(?)$	P_{11}	1708	174	···	···	···	···	···	···
$N(2100)$	P_{11}	2113	345	2131	394	2122	357	2116	360
$N(1720)$	P_{13}	1686	235	1706	219	1617	289	1641	252
$N(1520)$	D_{13}	1505	123	1505	129	1527	129	···	···
$N(1700)$	D_{13}	1805	130	1953	290	1809	129	···	···
$N(2080)$	D_{13}	1942	476	1960	270	···	···	···	···
$N(1675)$	D_{15}	1657	134	1657	136	1651	149	1620	108
$N(2200)$	D_{15}	2133	439	2134	375	2141	422	2130	401
$N(1680)$	F_{15}	1664	134	1665	135	1665	131	···	···
$N(1990)$	F_{17}	1990	303	1992	236	1979	362	···	···
$N(?)$	G_{17}	1740	270	1740	278	1774	148	···	···
$N(2190)$	G_{17}	2060	393	2051	333	1970	256	···	···

[a]Subthreshold.

IV. ANOMALY APPEARS

To make sure that the simple recipe given by Eq. (6) provides us with the true pole parameters (i.e. that we are searching for poles on the correct Riemann sheet [2,15,16]), we compared the results obtained by Eq. (6) with the values obtained by using the standard model-independent pole-extraction method: single-channel speed plot [3,17,18].

The speed-plot method relies on the following parametrization of the T-matrix amplitudes:

$$T(z) = \underbrace{\frac{r}{\mu - z}}_{\text{resonant part}} + \underbrace{\left(T(z) - \frac{r}{\mu - z}\right)}_{\text{smooth background}}, \tag{7}$$

where μ and r are pole position and pole residue, and the variable z stands for center-of-mass energy ($\sqrt{s}$).

In the speed-plot method, the resonance poles are in principle extracted from Eq. (7) with the (erroneous) assumption that the ''speed'' of the background can be completely neglected when compared to the speed of the resonant part. In principle, if one plots modulus of the speed of T (i.e. $|dT(z)/dz|$), the resonance produces a peak in this speed plot. In practice, there are known exceptions to that rule: the $N(1535)$ state, for instance, is actually hidden ''under the cloak'' of the ηN channel opening [3].

Using the speed-plot technique we have extracted the pole parameters from the coupled-channel partial waves of Ref. [7] for $\pi N \to \pi N$, $\pi N \to \eta N$, and $\eta N \to \eta N$ reactions. We summarized the results in Table II and compared them to the pole parameters of analytic continuation method. To our surprise, in some partial waves the obtained pole positions turned out to be different for different reactions and shifted with respect to the analytic continuation method by a few tens of MeV. That is in obvious contradiction with the input, because the pole positions are manifestly identical for all T-matrix elements by the very construction. Therefore, something was definitely wrong.

V. EXTRACTION METHOD TWO: REGULARIZATION

To understand and explain the unacceptable, we have thoroughly investigated the standard single-channel speed-plot technique and realized that it is not an exact method but only an approximation to a more general procedure. In the following, we develop an exact method for extracting the first-order pole from an arbitrary partial wave starting only with a very general set of assumptions. We call it the regularization method because its essence lies in the removal of the singularity and subsequent analysis of the obtained function. Finally, we compare the results obtained using the regularization method to results of speed-plot technique and analytic continuation.

Let there be an analytic function $T(z)$ of complex variable z which has a first-order pole at some complex point μ. The function $T(z)$ can be any of the T-matrix elements and variable z can be either Mandelstam s or center-of-

mass energy $\sqrt{s}$. In order to achieve a full correspondence with the speed-plot technique, from now on we are going to use the latter choice. Since all physical processes occur for real energy values, we are allowed to directly determine only $T(x)$ for x being a real number. To be able to successfully continue $T(x)$ into complex-energy plane (to search for its poles), we should regularize this function (i.e. remove the pole). In that case, any simple expansion of the regularized function would converge in the proximity of the removed pole.

The function $T(z)$ with a simple pole at μ is regularized by multiplying it with a simple zero at μ

$$f(z) = (\mu - z)T(z). \tag{8}$$

From this definition and Eq. (7), it is evident that the value of $f(\mu)$ is equal to the residue r of $T(z)$ at point μ. As we have the access to the function values on real axis only, the Taylor expansion of f is performed about some real x to give the value (residue) at the pole μ (where background is highly suppressed)

$$f(\mu) = \sum_{n=0}^{N} \frac{f^{(n)}(x)}{n!}(\mu - x)^n + R_N(x, \mu). \tag{9}$$

The expansion is explicitly written to the order N and the remainder is designated by $R_N(x, \mu)$. Using the mathematical induction one can show that the Nth derivative of $f(x)$, given by Eq. (8), is

$$f^{(n)}(x) = (\mu - x)T^{(n)}(x) - nT^{(n-1)}(x). \tag{10}$$

Insertion of this derivative into the Taylor expansion conveniently cancels all consecutive terms in the sum, except the last one

$$f(\mu) = \frac{T^{(N)}(x)}{N!}(\mu - x)^{(N+1)} + R_N(x, \mu), \tag{11}$$

where $T^{(N)}(x)$ is the Nth energy derivative of the T-matrix element. To simplify the notation, the pole can be written as a general complex number $\mu = a + ib$. Once the Taylor series converges the remainder $R_N(x, \mu)$ can be disregarded and the absolute value of both sides of Eq. (11) is given as

$$|f(\mu)| = \frac{|T^{(N)}(x)|}{N!}|a + ib - x|^{(N+1)}. \tag{12}$$

To keep the form as simple as possible, Eq. (12) is raised to the power of $2/(N + 1)$. After simple rearrangement of terms, in which we have collected the information on the T-matrix values on the right-hand side, and the information on the pole position and residue on the left-hand side, the elemental second-order polynomial emerges:

$$\frac{(a - x)^2 + b^2}{\sqrt[N+1]{|f(\mu)|^2}} = \sqrt[N+1]{\frac{(N!)^2}{|T^{(N)}(x)|^2}}. \tag{13}$$

This equation enables us to directly extract the pole position ($a = \mathrm{Re}\mu$, $b = \mathrm{Im}\mu$) and the absolute value of the function residue $|f(\mu)|$ from the T-matrix values at the real axis, namely, from the quantities directly attainable from the energy-dependent partial-wave analysis and evaluated at factual energy points x.

What we actually do is the following: we first find the Nth derivative of the T-matrix and then we calculate the right-hand side of Eq. (13). Observe that the *exact* knowledge of the right-hand side of Eq. (13) *in only three points* uniquely determines the pole parameters. The problem is that we must make a choice which particular three points to select. If points are too far from each other, there can be other singularities that would influence their values. On the other hand, if they are too close, numerical problems might occur. There are basically two ways out: either (i) take various three-point sets, evaluate the right-hand side of Eq. (13), solve the equation for pole parameters, and make a statistical analysis of obtained results; or (ii) fit the right-hand side of Eq. (13) with the three parameter parabolic function. We have chosen the latter option, since it is more straightforward, and have obtained fitting parameters.

Up to now, we have shown how to obtain the real part of the pole a, the square of the imaginary part b^2, and the magnitude of the residue $|f(\mu)|$. The full complex residue $f(\mu)$ is obtained from Eq. (11) when convergence is achieved. At this point, the R_N term can be neglected. Then, $f(\mu)$ is evaluated by setting $x = \mathrm{Re}\mu$. Because all resonances have negative imaginary parts, the sign of b is taken to be negative. If the sign of b is taken to be the opposite (i.e. positive) the phase of $f(\mu)$ would be changing by π for running values of N.

In a form consistent with Ref. [5], the magnitudes and phases of residues are calculated as

$$|r| = |f(\mu)|, \qquad \tan\theta = \mathrm{Im}f(\mu)/\mathrm{Re}f(\mu). \tag{14}$$

The standard speed-plot method turns out to be the regularization method in the first-order approximation! [To get the speed plot, one should reduce the expansion given by Eq. (9) to $N = 1$ term.]

As a concluding remark, let us say that we *did not have* to make any assumptions on the *functional form* of the T-matrix under consideration, as was the case with the N/D method. In the N/D method, the T-matrix is assumed to be of Breit-Wigner form in a wider energy range around the singularity; and only the total width is corrected with the energy-dependent function in order to account for the proximity of inelastic channel openings. In the regularization method we have not assumed any functional form of the T-matrix whatsoever but have only eliminated the simple pole by multiplying the analyzed function with the simple zero $(\mu - z)$.

VI. RESULTS

Using the speed-plot technique we have extracted pole parameters from the coupled-channel amplitudes of

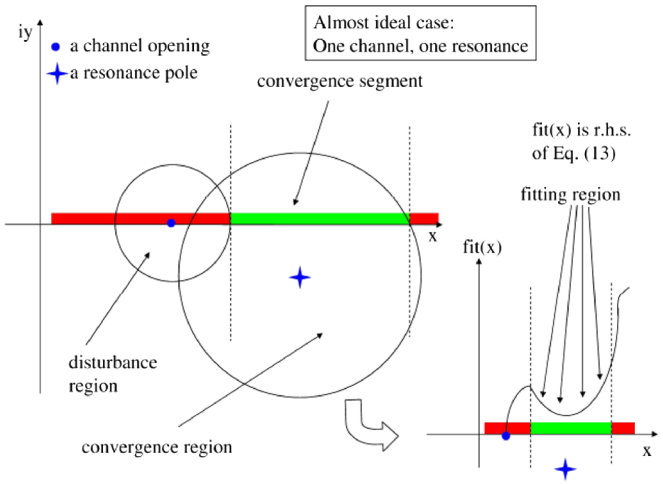

FIG. 1 (color online). A very simplified example: one resonance and one channel opening.

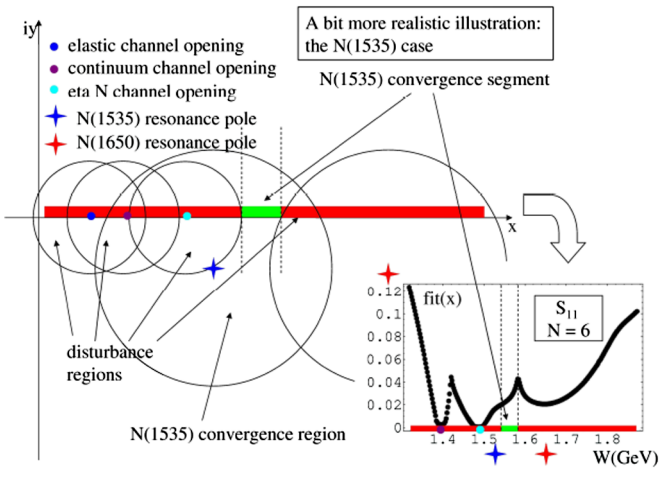

FIG. 2 (color online). The illustration of the regularization method in the case of $N(1535)$ S_{11} resonance.

Ref. [7]. The obtained pole positions were different for each process and shifted with respect to analytic continuation method by a few tens of MeV. We claim that this is unacceptable and demands to be understood, so we repeat a similar analysis using the regularization method instead.

Despite being mathematically straightforward, the application of the regularization method requires additional explanation when using Eq. (13). Namely, we have to answer the two major questions: (i) when to stop the Taylor series expansion in Eq. (9) (to determine N) and (ii) which energy interval of input data—given by the right-hand side of Eq. (13)—to fit.

The answer is simple for the ideal case when we have no additional poles and no channel openings. However, in the real world we are faced with the situation where we have more then one resonance per partial wave and numerous inelastic channel openings. That makes life complicated and we have to invent the criteria.

Let us illustrate how the method works in principle.

TABLE III. The comparison of N^* resonance pole parameters obtained by the analytic continuation method, and the regularization method for πN, $\eta N \to \eta N$, and $\pi N \to \eta N$ processes. Numbers in subscript are the expansion order required to obtain convergent result.

Resonance		Analytic continuation		Regularization method					
				$\pi N \to \pi N$		$\pi N \to \eta N$		$\eta N \to \eta N$	
N^*	L_{2I2J}	Reμ (MeV)	-2 Imμ (MeV)	Reμ (MeV)	-2 Imμ (MeV)	Reμ (MeV)	-2 Imμ (MeV)	Reμ (MeV)	-2 Imμ (MeV)
$N(1535)$	S_{11}	1517	190	$1522_{(7)}$	$146_{(7)}$	...	...	...	...
$N(1650)$	S_{11}	1642	203	$1647_{(7)}$	$203_{(7)}$	$1645_{(10)}$	$211_{(10)}$	...	...
$N(2090)$	S_{11}	1785	420	...	...	...	...	...	...
$N(1440)$	P_{11}	1359	162	$1354_{(8)}$	$162_{(8)}$	ST[a]	ST[a]	ST[a]	ST[a]
$N(1710)$	P_{11}	1728	138	$1729_{(8)}$	$150_{(8)}$	$1733_{(5)}$	$133_{(5)}$	$1728_{(7)}$	$142_{(7)}$
$N(?)$	P_{11}	1708	174	...	...	...	...	...	...
$N(2100)$	P_{11}	2113	345	$2120_{(6)}$	$347_{(6)}$	$2120_{(6)}$	$347_{(6)}$	$2120_{(6)}$	$347_{(6)}$
$N(1720)$	P_{13}	1686	235	$1691_{(5)}$	$235_{(5)}$	$1691_{(5)}$	$234_{(5)}$	$1691_{(5)}$	$235_{(5)}$
$N(1520)$	D_{13}	1505	123	$1506_{(4)}$	$124_{(4)}$	...	...	...	...
$N(1700)$	D_{13}	1805	130	$1806_{(5)}$	$132_{(5)}$	$1806_{(4)}$	$130_{(4)}$	...	...
$N(2080)$	D_{13}	1942	476	...	...	...	...	...	...
$N(1675)$	D_{15}	1657	134	$1658_{(5)}$	$138_{(5)}$	$1657_{(3)}$	$137_{(3)}$	$1658_{(5)}$	$138_{(5)}$
$N(2200)$	D_{15}	2133	439	$2145_{(6)}$	$439_{(6)}$	$2144_{(4)}$	$435_{(4)}$	$2144_{(6)}$	$438_{(6)}$
$N(1680)$	F_{15}	1664	134	$1666_{(4)}$	$136_{(4)}$	$1665_{(3)}$	$136_{(3)}$	...	...
$N(1990)$	F_{17}	1990	303	$2016_{(7)}$	$318_{(7)}$	$2015_{(6)}$	$322_{(6)}$	...	...
$N(?)$	G_{17}	1740	270	$1749_{(6)}$	$280_{(6)}$	$1748_{(6)}$	$281_{(6)}$	...	...
$N(2190)$	G_{17}	2060	393	$2068_{(5)}$	$389_{(5)}$	...	...	...	...

[a]Subthreshold.

TABLE IV. Residues and phases.

	Review of Particle Physics[a] [5] elastic pole residues			Regularization method	
N^*	L_{2I2J}	$\|r\|$ (MeV)	θ (°)	$\|r\|$ (MeV)	θ (°)
$N(1535)$	S_{11}	77	15	19	−146
$N(1650)$	S_{11}	56	−56	84	−58
$N(2090)$	S_{11}	40	0		
$N(1440)$	P_{11}	43	−101	47	−95
$N(1710)$	P_{11}	11	−176	52	−156
$N(?)$	P_{11}	...	...	...	...
$N(2100)$	P_{11}	14	35	31	−59
$N(1720)$	P_{13}	14	−124	19	−112
$N(1520)$	D_{13}	34	−8	36	−14
$N(1700)$	D_{13}	6	0	7	−36
$N(2080)$	D_{13}	20	50	...	...
$N(1675)$	D_{15}	28	−25	25	−20
$N(2200)$	D_{15}	20	−90	22	−71
$N(1680)$	F_{15}	40	−14	45	−26
$N(1990)$	F_{17}	9	−60	8	−25
$N(?)$	G_{17}	...	...	6	−86
$N(2190)$	G_{17}	46	−31	34	−30

[a]Since RPP does not provide estimates for residues and phases, we averaged published values with uniform weight.

Figure 1 shows a very simplified example: we analyze the case with one resonance and one channel opening. The channel opening determines (restricts) the radius of convergence of the Taylor expansion, so the input data, i.e. the right-hand side of Eq. (13), have to be restricted to the convergence segment. In practice we do the following: we construct the right-hand side of Eq. (13) for $N = 1$, select by ''naked eye'' a parabola-looking data set. Then we fit the left-hand side to the data in order to extract the set of pole parameters a, b, and $|f(\mu)|$. We perform a series of fits, starting with $N = 1$, and wait until the resulting parameter set value stabilizes. Once the stability is achieved, we declare that we have found the pole.

In reality, we have applied the identical procedure, but choosing the correct parabola-looking subset of data was the main source of indetermination.

The data set for the right-hand side of Eq. (13) was produced from partial-wave amplitudes of Ref. [7]. For all three processes, $T^{(N)}(x)$ was obtained by numerical differentiation of energy-dependent partial waves. A 2 MeV step size yielded a stable solution. The succession of fits was performed by increasing the number of Taylor series terms and the expansion is stopped when the extracted parameter set settles down. We usually needed 3–8 terms in order to achieve the reasonable convergence and the higher orders were needed only to confirm the convergence.

The pole parameters attained in this way, with the subscript (N) denoting the number of required Taylor series terms, are for all three calculated processes (in identical form as in Table II) given in Table III.

The disagreement of the speed-plot recipe ($N = 1$ regularization method term) and the values obtained when using the analytic continuation method is eliminated, therefore we conclude that the simple recipe given by Eq. (6) indeed chooses the poles on the correct Riemann sheet. The explanation of the motivating problem (the anomaly that the speed-plot technique gives different results for different reactions) is obvious as well from Table III: the final result is stable with respect to the choice of different channel processes. The anomaly was due to the fact that the speed-plot technique is the first-order approximation of the regularization method. The full calculation (regularization method) gives the same answers for all channels (provided that the result can be obtained using this method).

The speed-plot technique works fine for relatively isolated poles. When a pole is surrounded by other poles and/or inelastic channel openings, as is the case for $N(1535)$ S_{11} resonance, the first approximation of the regularization method (speed plot) is not sufficient and one has to take higher derivatives into consideration. The problem for this notoriously problematic resonant state is illustrated in Fig. 2.

Residues and phases for N^* resonances are given in Table IV. Since the RPP [5] does not provide averages for the residue parameters, values from each residue table in Ref. [5] were averaged with uniform weight.

VII. CONCLUSIONS

The improved analytic continuation method (Pietarinen-like expansion of the channel propagator), which has been developed for the coupled-channel formalism, provides pole positions quickly and precisely while avoiding problems with numerical principal value integration and interpolation. The obtained pole positions are in accordance with RPP values.

The developed regularization method represents an improvement of contemporary single-channel pole-extraction methods. We demonstrate that it successfully finds resonance pole parameters from an energy-dependent T-matrix in a model-independent way, i.e. without having to assume a specific T-matrix functional form.

Furthermore, the regularization method can be generally applied to most analytic functions that have a simple pole and values known on any line segment reasonably close to the pole.

The single-channel speed-plot recipe is only the first-order term of the regularization method and it should be applied with special care.

The elastic pole residues are in accordance with those given in RPP. Since there are still no elastic residue estimates in RPP, we strongly advocate making them in future editions.

[1] R. G. Newton, *Scattering Theory of Waves and Particles* (Springer-Verlag, Berlin, 1982).
[2] B. H. Bransden and R. G. Moorhouse, *The Pion Nucleon Systems* (Princeton University, Princeton, NJ, 1973).
[3] G. Höhler, πN Newsletter **9**, 1 (1993).
[4] R. Workman, Phys. Rev. C **59**, 3441 (1999).
[5] S. Eidelman *et al.*, Phys. Lett. B **592**, 1 (2004).
[6] R. E. Cutkosky, C. P. Forsyth, R. E. Hendrick, and R. L. Kelly, Phys. Rev. D **20**, 2839 (1979).
[7] M. Batinić, I. Šlaus, A. Švarc, and B. M. K. Nefkens, Phys. Rev. C **51**, 2310 (1995); M. Batinić *et al.*, Phys. Scr. **58**, 15, (1998).
[8] E. Pietarinen, Nuovo Cimento Soc. Ital. Fis. **12A**, 522 (1972).
[9] G. F. Chew and S. Mandelstam, Phys. Rev. **119**, 467 (1960).
[10] J. A. Oller and E. Oset, Phys. Rev. D **60**, 074023 (1999).
[11] V. V. Anisovich, Int. J. Mod. Phys. A **21**, 3615 (2006).
[12] S. M. Flatté, Phys. Lett. **63B**, 224 (1976).
[13] T. P. Vrana, S. A. Dytman, and T.-S. H. Lee, Phys. Rep. **328**, 181 (2000).
[14] I. Ciulli, S. Ciulli, and J. Fisher, Nuovo Cimento **23**, 1129 (1962).
[15] R. J. Eden and J. R. Taylor, Phys. Rev. **133**, B1575 (1964).
[16] D. Morgan and M. R. Pennington, Phys. Rev. Lett. **59**, 2818 (1987).
[17] D. J. Herndon, A. Barbaro-Galtieri, and A. H. Rosenfeld, Lawrence Radiation Laboratory Report No. UCR-20030, 1960.
[18] O. Hanstein, D. Drechsel, and L. Tiator, Phys. Lett. B **385**, 45 (1996).